IOP Conf. Series: Materials Science and Engineering **233** (2017) 012016 doi:10.1088/1757-899X/233/1/012016

Axial pico turbine – construction and experimental research

G. Peczkis[1], Z Goryca[2], A Korczak[1]

[1]Politechnika Śląska, St. Konarski 18 Street, 44-100 Gliwice, Poland
[2]Kielce University of Technology, Aleja Tysiąclecia Państwa Polskiego 7, PL- 25314 Kielce, Poland

E-mail: peczkis@wp.pl

Abstract: The paper concerns axial water turbine of power equal to 1 kW. The example of axial water turbine constructional calculations was provided, as well as turbine rotor construction with NACA profile blades. The laboratory test rig designed and built to perform measurements on pico turbine was described. The turbine drove three-phase electrical generator. On the basis of highest efficiency parameters, pico turbine basic characteristics were elaborated. The experimental research results indicated that pico turbine can achieve maximum efficiency close to the values of larger water turbines.

1. Introduction

The most prevalent natural hydrological conditions in the lowlands, predominating in Central Europe, are characterized by low heads in small and medium watercourses flows rates. Such conditions favor use of water head energy by means of water wheels, Banks - Mitchell turbines and propeller turbines [3]. Rational locations for these turbines possible installations are largely dispersed, so that their powers do not usually exceed several to several dozen kW.

Classification of hydropower plants, according to capacity installed:

- ✓ Large hydropower plants > 10 MW,
- ✓ Small hydropower plants (MEW) < 10 MW,

including:

- ✓ mini < 1 MW,
- ✓ micro < 100 kW,
- ✓ pico < 5 kW.

The paper concerns construction, experimental research and assessment of pico turbine performance, which is designed to work in following conditions:

- water courses with low head and low discharge,
- regeneration,

Moreover, the investigated construction can be concerned as the model machine for the higher capacity turbines.

2.Water turbines efficiency

The decision concerning constructing and building a power machine results, among others, from efficiency that it can achieve. In Figure 1. the chart shows hydraulic losses, which for turbines with impeller diameter <0,46 m grow progressively.

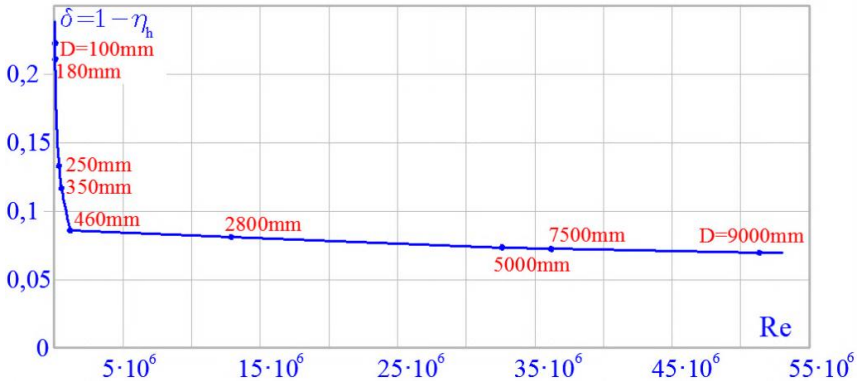

Figure 1. Hydraulic losses in axial turbine as function of Reynolds number [A.M. Chrystjakov].

Reynolds number for propeller turbines is as follows [1]:

$$Re = \frac{d_3\sqrt{2gH}}{\nu} \tag{1}$$

where: d_3 – propeller turbine outlet diameter, m

H – water head, m

ν – kinematic viscosity, $\frac{m}{s^2}$

g – gravitational acceleration, $\frac{m}{s^2}$

According to Figure 1, the pico turbines are characterized by additional hydraulic losses, resulting from low Reynolds numbers. The empirical investigation is justified, as it aims to minimize the total loss during machine performance. The measurements on pico turbines can be carried out on the machine with scaling factor 1. On the basis of dynamic similarity the results of the measurements can be used as the model test in designing process of geometrical similar, higher capacity machines.

For the specific speed $n_b \geq 0{,}33$ and discharge $Q < 0{,}65\frac{m^3}{s}$ total efficiency η_C can be obtained from:

$$\eta_C = \sqrt{\left(\frac{Q}{0{,}048}\right)^{0{,}07} - \left(-0{,}722 - \log n_b\right)^5} - \xi = 0{,}814 \tag{2}$$

where $\xi = 0{,}2$ for one stage turbine.

The total efficiency obtained from experiment investigation was proved by result of calculation conducted according to cited formulas.

The hydraulic efficiencies η_h of a turbine cannot be obtained from experiment results, but they are necessary for constructional calculations. They are determined according to following formulas proposed by:

Wislicenus
$$\eta_h = \sqrt{\eta_C} - (0{,}02 \div 0{,}06) = 0{,}88 \div 0{,}84 \tag{3}$$

Lomakin
$$\eta_h = 1 - \frac{0{,}42}{\left[\log\left(4{,}2 \cdot 10^3 \sqrt[3]{\frac{Q}{60n}}\right) - 0{,}172\right]^2} = 0{,}85 \tag{4}$$

Jekat $$\eta_h = 1 - \frac{0{,}8}{(158503Q)^{0{,}25}} = 0{,}86 \quad (5)$$

Michajlow $$\eta_h = 0{,}7 + 0{,}0835 log\left(4 \cdot 10^3 \sqrt[3]{\frac{Q}{60n}}\right) = 0{,}84 \quad (6)$$

The research described in this article aims to verify the accuracy of these formulas on the basis of empirical investigation of machine performance.

Due to the diameter of pico turbine $d<0{,}25m$ for construction calculations the assumption of $\eta_h = 0{,}75$ was done.

3. Determination of principle dimensions of axial turbine rotor

During construction process the highest efficiency operating conditions were assumed, what was proved in empirical investigation:

flow rate $Q = 4\frac{m^3}{min}$, head $H = 2{,}m$, rotational speed $n = 850\frac{obr}{min}$

The dynamic specific speed n_s from formula:

$$n_s = 3{,}65n\frac{\sqrt{Q}}{H^{0{,}75}} = 476 \quad (7)$$

The specific speed n_b, used in following calculations [3]:

$$n_b = \frac{n_s}{1213{,}9} = 0{,}392 \quad (8)$$

The value of specific speed indicates that the investigated turbine is an axial one. The power on turbine shaft is defined as:

$$P = \frac{gpQH}{\eta_h} \quad (9)$$

Meridional velocity:

$$c_m = K_m\sqrt{2Y_N} = 2{,}07\frac{m}{s} \quad (10)$$

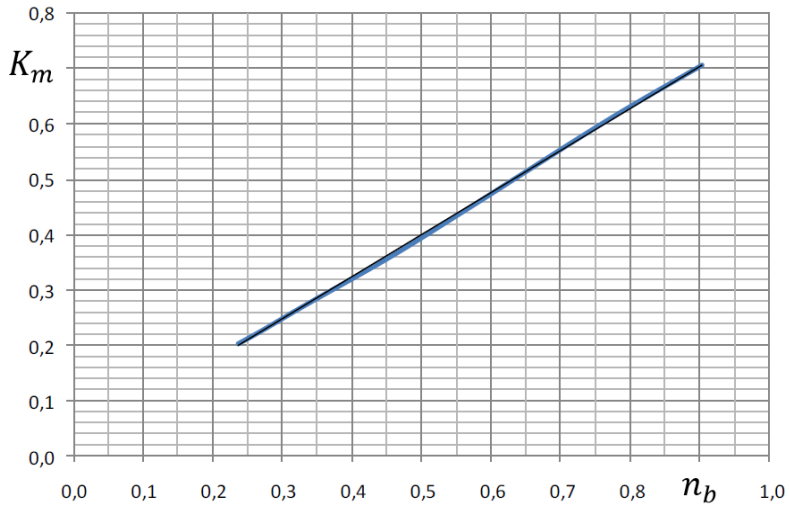

Figure 2. The relation between the specific speed and Km coefficient.

The coefficient Km for the average meridional velocity can be obtained from the chart (Figure 2) or by the formula:

$$K_m = 0{,}0688 + 0{,}733 n_b^{1{,}1} = 0{,}331 \tag{11}$$

Turbine rotor diameter ratio can be calculated from:

$$\frac{D_n}{D_A} = 0{,}63 - 0{,}346\left(n_b - 0{,}25\right) = 0{,}584 \tag{12}$$

Meridional velocity:

$$c_m = \frac{Q + \Sigma Q_z}{\frac{\pi}{4}\left(D_n^2 - D_A^2\right)} = 2{,}11\frac{m}{s} \tag{13}$$

The diameter D_A can be determined:

$$D_A = \sqrt{\frac{4\left(Q + \Sigma Q_z\right)}{\pi c_m\left[1 - \left(\frac{D_n}{D_A}\right)^2\right]}} = 0{,}228m \tag{13a}$$

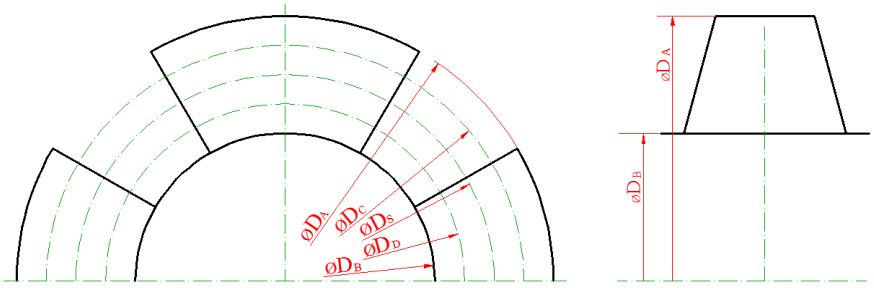

Figure 3. The diameters of designed turbine rotor.

With the assumption of constant meridional velocity and dividing the flow between the diameters $D_{A, C, S, D, B}$ shown in Figure 3 equally, these diameters can be calculated from:

$$D_S = \sqrt{\frac{D_A^2 + D_n^2}{2}} = 0{,}187m \qquad D_C = \sqrt{\frac{D_S^2 + D_A^2}{2}} = 0{,}208m \qquad D_D = \sqrt{\frac{D_B^2 + D_S^2}{2}} = 0{,}162m \quad (14\ \text{a,b,c})$$

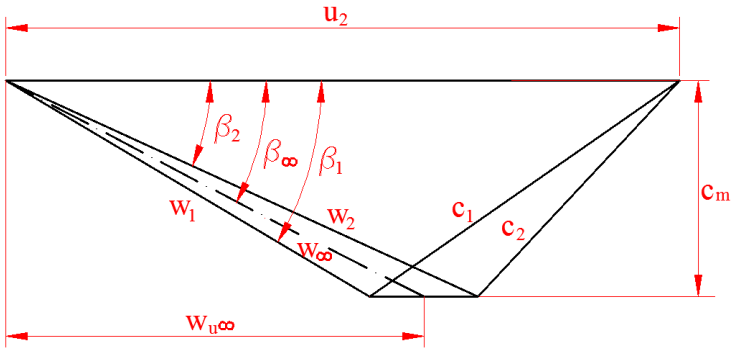

Figure 4. Velocity triangles of axial rotor.

The change of tangential component of rotor velocity on diameter D is equal to:

$$c_{u1} - c_{u2} = \frac{\Gamma}{2\pi r} = 2{,}19\frac{m}{s} \tag{15}$$

Where Γ- circulation around rotor blade foil, which is defined as:

$$\Gamma = 2\pi r \frac{\eta_h g H}{u} = 1{,}28 \tag{16}$$

The average tangential component of relative velocity (Figure 4) is:

$$w_{u\infty} = \frac{w_{u1} + w_{u2}}{2} = u - \frac{gH}{2\pi u \eta_h} \tag{17}$$

The change of tangential component of relative velocity:

$$\Delta w_u = w_{u2} - w_{u1} \tag{18}$$

Assuming $c_{m\infty} = c_m$ it can be stated:

$$\beta_\infty = arctg \frac{c_{m\infty}}{w_{u\infty}} \tag{19}$$

The theoretical angle β_∞, has to be increased by an additional angle $\Delta\beta = \Delta\delta$ and as a result, the angle of attack $\beta_e = \beta_\infty + \Delta\beta = 15{,}7^\circ$ is obtained for rotor outer diameter. The angle β_e for other streamlines is calculated in the same way.

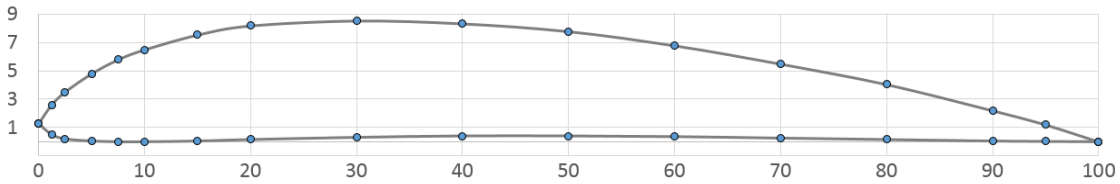

Figure 5. The shape of NACA 2412 profile, used to design the blades.

4. Axial turbine blade design process

The shapes of turbine blades were designed on basis of NACA 2412 foil (Figure 5). The foil is described by characteristic dimensions ratio. The profile sketch was drawn on XY plane. Next, the profile chord was increased, with proportions kept. Then it was decided to change the proportions, so that the thickness of blade was reduced to technologically possible minimum. The obtained blade profile no longer kept the proportions of original NACA 2412 profile, particularly the ratio between the maximum thickness and chord length was interrupted. In Figure 6 the different rotor diameters profiles obtained from this method are shown.

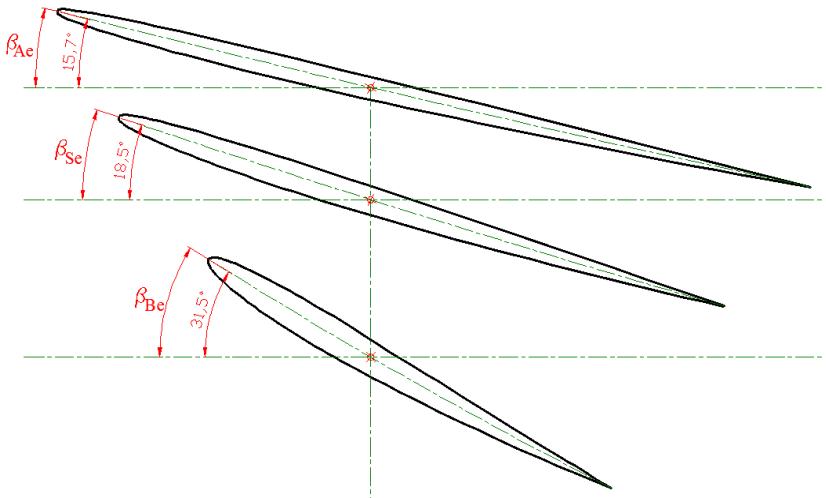

Figure 6. NACA profiles for different rotor diameters.

Next constructional work, performed in XYZ coordination system, included connecting different diameters profiles with one surface and blade root, which enables proper, explicit connection with the rotor hub. The shape of blade in shown in Figure 7. In the investigated construction, the blade is placed on cylinder hub, so that the angle of attack changes are not possible. The blade placing on a hub results in one configuration, shown in Figure 8. The change of blade angles is possible only in case of at least partial spherical hub. Presented turbine rotor blade was used in experimental research. It was made of PA6 aluminum alloy, with use of multi axis milling technique.

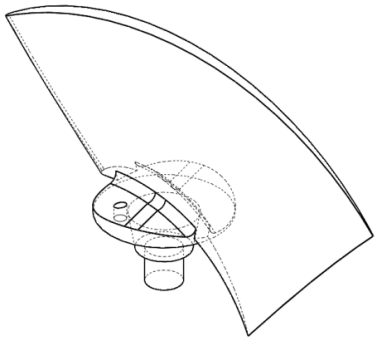

Figure 7. The blade obtained from profiles connection. The blade root embedded on conical fitting.

The processing of these types of elements meets the problem of deflection and vibration of processed material under the cutter pressure (due to the low stiffness). During the serial production it should not be a problem, as the blades would be a casting or a forging, but it was a difficulty during prototype elements production.

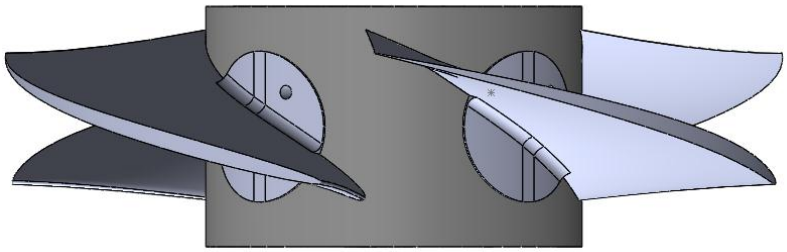

Figure 8. The view of the hub with 4 blades.

5. The water turbine prototype

For investigation purposes it was decided to build an axial turbine connected to generator with a clutch (see Figure 9). The ceramic bushing with water passing through the turbine as a lubricating fluid was used. This solution provides very low mechanical losses in bearing. However, this type of bearings has low resistance to resilience. The lack of axial bearing in a scheme shown in Figure 9 is a result of axial forces transfer by means of generator's bearing. In this situation, it is necessary to use an untypical clutch, that rotating part of the turbine is hung on.

At the inlet to the turbine rotor the stator with profiled blades was installed. The stator blades have the regulated angle. The geometry of stator blades is not included in the paper.

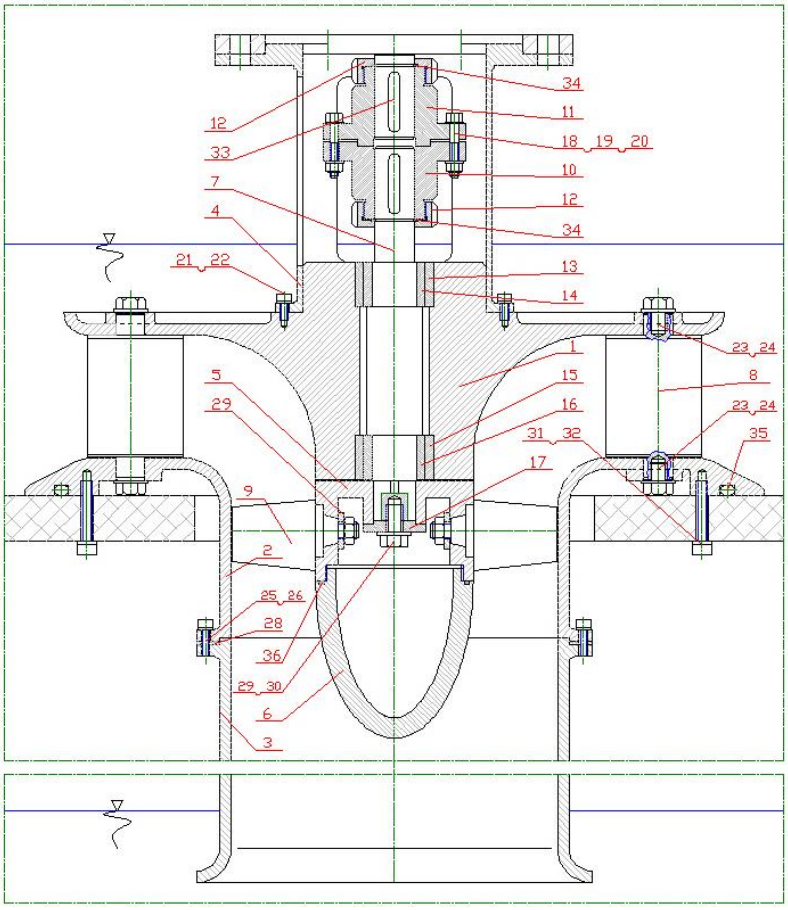

Figure 9. The scheme of the turbine. Four blade rotor version.

6. The turbine test rig

The scheme of pico turbine test rig is shown in Figure 10. Taking into consideration specific speed of the turbine and after literature research, it was decided to build symmetrical inflow channel with one crosswise rib, that prevents water circulation at the turbine inlet. The lack of rib resulted in cyclic vortex appearance, which caused air inflow to the turbine.

The water turbine test rig was designed for only one size of the turbine. The proposed shape of inflow channel can be installed under target conditions (e.g. a river estuary). Water was delivered to the circuit by means of a centrifugal pomp. A draft tube of constant diameter was manufactured for measurement purpose. In future work, it is planned to apply a diffuser with appropriate angle.

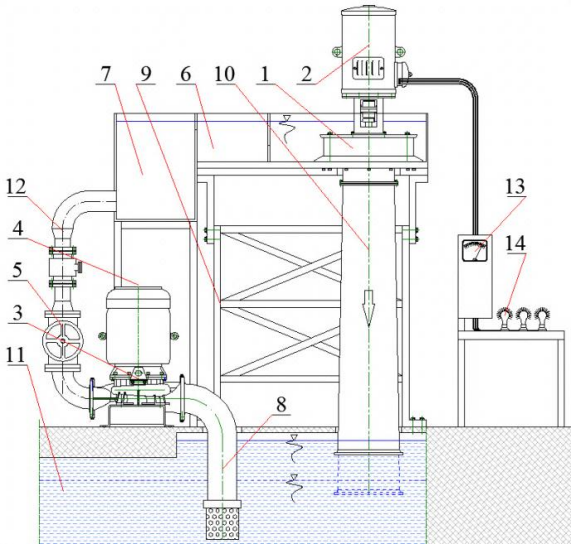

Figure 10. The scheme of water turbine and three – phase generator test rig. 1- turbine, 2- generator, 3-supplying pump, 4- pump motor, 5- valve, 6 – inflow channel, 7- buffer, 8 – suction pipe, 9 – load-bearing construction 10, - draft tube 11 – underfloor tank, 12 – discharge pipe, 13 – electrical meter, 14 – electrical resistor.

6.1 Performing the experiment

To obtain turbine performance curves it is necessary to perform the measurements at constant rotational speed. During the measurements series of points with different operating conditions were determined. The further analysis included highest efficiency operating point.

The view of the test rig is shown in Figure 11. Water was pumped from a tank located under the floor by means of the pump with smooth rotational speed regulation. It flowed evenly to the turbine through the inflow channel. To reduce the flow rate of the water (to lower water velocity), the flow was directed to a tank and then it overflowed to the inflow channel. After passing the turbine water was flowing through the draft tube back to the underfloor tank. Regulation of water flow rate was performed by changing the rotational speed of supplying pump. Regulation of water head was done by changing the water level in the underfloor tank. Electricity produced by three - phase turbine generator supplies set of lightbulbs connected in a wye system. The measurements of electrical parameters were also carried out. To increase the load of each phase the additional lightbulbs were added serially and also in parallel.

Figure 11. View of the measurement system during the experiment.

6.2 Measurements results

The efficiency of water turbine and its generator is derived from flow rate Q, head H and electrical power P_e measurement results. Measurements of flow rate were provided by means of electromagnetic flowmeter. The value of head was defined as a distance between water level in the inflow channel and water level in the underfloor tank. To measure the electrical power an universal meter was used. It indicated voltage, current and phase angles (three-phase system).

6.2.1. Mechanical parameters measurement

The Best Efficiency Point for the investigated pico turbine, at specific head H, was characterized by following parameters:

Head $H = 2{,}18\ m$,
Flow rate: $Q = 4{,}22\ m^3/min$,
Rotational speed: $n = 859\ rev/min$,
The average water axial velocity at turbine outlet:

$$V_{sr} = 1{,}723\frac{m}{s}$$

The measured work parameters indicate the hydraulic power of water flow:

$$P_h = Q\,\rho\,g\,H = 1504\ W \tag{20}$$

They also indicate the specific speed of the turbine [4]:

$$n_s = 1{,}167n\frac{\sqrt{P_h}}{H^{5/4}} = 464{,}1 \tag{21}$$

where: n [rev/min], P_h [kW], H [m].

6.2.2 Measurements of generator's electrical parameters

The measurements were taken at electrical side of the generator driven by the turbine. The generator was loaded by electrical resistors. The three – phase generator, at rotational speed n = 859 rev/min produced electrical current of following parameters:

Voltage U = 458 V,
Current I = 1,65 A,
Electrical power:

$$P_e = \sqrt{3}UI\cos\varphi = 1050\,W \tag{22}$$

Shaft power :

$$P = \frac{P_e}{\eta_e} = \frac{1050}{0{,}85} = 1123{,}53W \tag{23}$$

The efficiency of turbine - generator system was derived from water hydraulic power and generator's electrical power:

$$\eta_a = \eta_T\eta_G = \frac{P_e}{P_h} = 0{,}698 \tag{24}$$

The efficiency of pico turbine is defined as:

$$\eta_T = \frac{\eta_a}{\eta_G} = 0{,}821 \tag{25}$$

where η_G – generator efficiency was determined on basis of its characteristic shown in Figure 12.

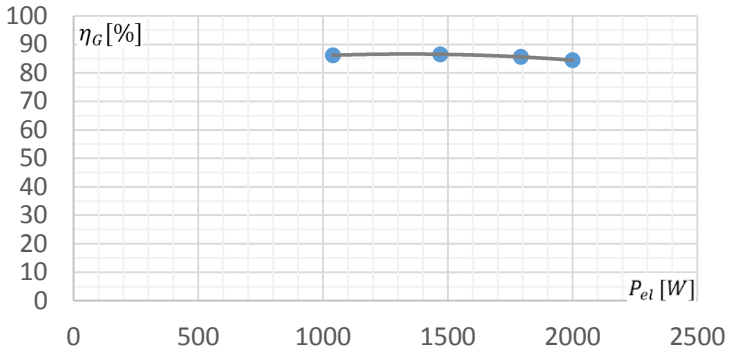

Figure 12. Generator efficiency η_G as a function of load P_{el}.

6.3 The basic performance curves for pico turbine

On the basis of Best Efficiency Point parameters for the investigated turbine and typical performance curves for water turbines the characteristics for pico turbine were elaborated. They are depicted in Figure 13.

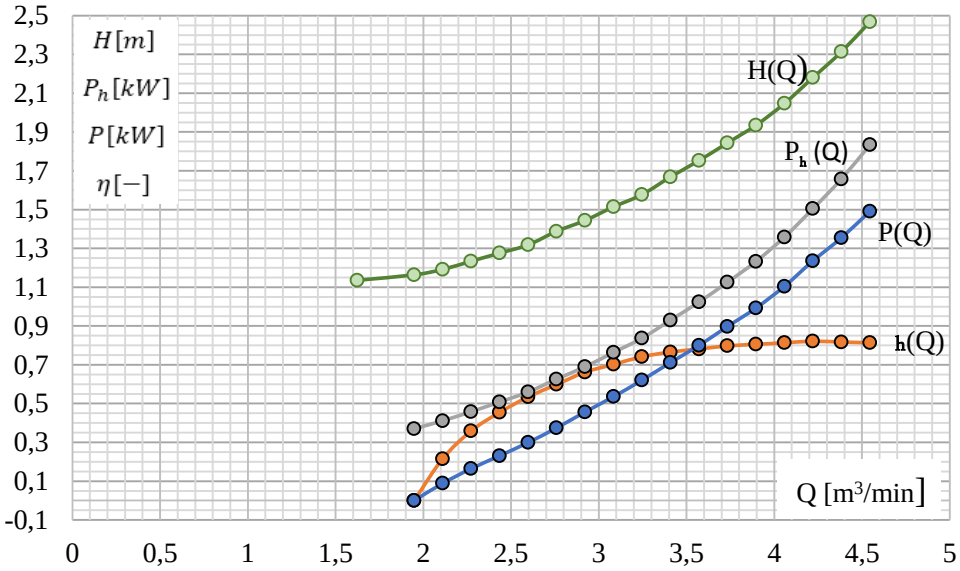

Figure 13. The investigated pico turbine characteristics, elaborated from Best Efficiency Point parameters.

7. Conclusions

1. The experimental research showed that efficiency of a pico turbine of rotor diameter d = 228 mm can be as high as it is indicated in Equation 2 (with no additional losses shown in Figure 1) under following conditions: precise elements production and pico turbine assembly and application of appropriate bearings.
2. The algorithm described in [2] was used in hydraulic and constructional calculations. The calculations results were in good agreement with turbine parameters obtained during the experiment.
3. The application of NACA 2412 as rotor blades profiles was a good choice, which proves the conclusion 1.
4. The use of ceramic bearings, lubricated and cooled by water passing through the turbine was also a good choice. Moreover, they had low rolling resistance.
5. The application of an inflow channel with one crosswise rib (with dimensions recommended in [1]) enables to provide stable flow rate through the turbine.
6. As it was mentioned in Introduction, pico turbine investigation results can be applied during production of this type of turbines and as model machine investigation for higher capacity turbines.

7. Stabilization of parameters after generator load change (and turbine load consequently) was quite time consuming. It was decided to build a different regulation system in further research, so that the turbine load can be changed smoothly, with simultaneous shaft power measurement.

References

[1] W Krzyżanowski 1971 *Turbiny wodne, konstrukcja i zasady regulacji* (Warszawa: WNT)
[2] Varchola M, Hlbočan P 2016 *Hydraulický návrh axiálneho stroja* (Bratislava: SUT)
[3] Korczak A, Rduch J 2009 *Energetyka wodna w Polsce, stan i perspektywy rozwoju* Monografia Komitetu Inżynierii Środowiska PAN, III Kongres Inżynierii Środowiska (Lublin) **3** pp 33-59
[4] Kowaliew N N 1971 *Gidroturbiny* (Leningrad: Maszinostrojenije) p 584